Decline in Mitochondrial Bioenergetics and Shift to Ketogenic Profile in Brain During Reproductive Senescence

Jia Yao[a], **Ryan T. Hamilton**[a], **Enrique Cadenas**[a], and **Roberta Diaz Brinton**[a,b]

[a]Department of Pharmacology and Pharmaceutical Sciences, School of Pharmacy, University of Southern California, Los Angeles, California 90033

[b]Program in Neuroscience, University of Southern California, Los Angeles, 90089

Abstract

Background—We have previously demonstrated that mitochondrial bioenergetic deficits precede Alzheimer's pathology in the female triple transgenic Alzheimer's (3xTgAD) mouse model. Herein, we sought to determine the impact of reproductive senescence on mitochondrial function in the normal non-transgenic (nonTg) and 3xTgAD female mouse model of AD.

Methods—Both nonTg and 3xTgAD female mice at 3,6,9, and 12 months of age were sacrificed and mitochondrial bioenergetic profile as well as oxidative stress markers were analyzed.

Results—In both nonTg and 3xTgAD mice, reproductive senescence paralleled a significant decline in PDH, and Complex IV cytochrome c oxidase activity and mitochondrial respiration. During the reproductive senescence transition, both nonTg and 3xTgAD mice exhibited greater individual variability in bioenergetic parameters suggestive of divergent bioenergetic phenotypes. Following transition through reproductive senescence, enzymes required for long-chain fatty acid (HADHA) and ketone body (SCOT) metabolism were significantly increased and variability in cytochrome c oxidase (Complex IV) collapsed to cluster at a ~40% decline in both the nonTg and 3xTgAD brain which was indicative of alternative fuel generation with concomitant decline in ATP generation.

Conclusions—These data indicate that reproductive senescence in the normal nonTg female brain parallels the shift to ketogenic/fatty acid substrate phenotype with concomitant decline in mitochondrial function and exacerbation of bioenergetic deficits in the 3xTgAD brain.

General Significance—These findings provide a plausible mechanism for increased life-time risk of AD in postmenopausal women and suggest an optimal window of opportunity to prevent or delay decline in bioenergetics during reproductive senescence.

Keywords

Mitochondria; Bioenergetics; Reproductive Senescence; Alzheimer's disease; estrogen

---

Corresponding Author: Roberta Diaz Brinton, Ph.D., Pharmacology & Pharmaceutical Sciences, University of Southern California, Pharmaceutical Sciences Center, 1985 Zonal Avenue PSC502, Los Angeles, CA 90089, Voice: 323-442-1428, FAX: 323-442-1489, rbrinton@usc.edu.

1. Introduction

The essential role of mitochondria in cellular bioenergetics and survival has been well established [1–3]. Further, mitochondrial dysfunction has been suggested to play a pivotal role in neurodegenerative disorders, including Alzheimer's disease (AD) [1, 4–5]. It has been shown that brain metabolism is declined in AD patients at least a decade before disease diagnosis [1, 6–9]. Dysfunction in glucose metabolism, bioenergetics and mitochondrial function are consistent antecedents to development of Alzheimer pathology [10–18]. Recently we demonstrated that mitochondrial bioenergetic deficits precede Alzheimer's pathology in the female triple transgenic mouse model of Alzheimer's disease (3xTgAD) [7]. These antecedent declines in brain metabolism indicate a potential causal role of mitochondrial bioenergetics in AD pathogenesis and disease progression.

Basic science analyses indicate that the endogenous estrogen, 17β-estradiol (E2), significantly increased glucose uptake, glucose metabolism, insulin growth factor signaling and the energetic capacity of brain mitochondria by maximizing aerobic glycolysis (oxidative phosphorylation coupled to pyruvate metabolism) [1, 6, 19]. The enhanced aerobic glycolysis in the aging brain would be predicted to prevent conversion of the brain to using alternative sources of fuel such as the ketone body pathway characteristic of AD [1, 6]. The ability of estrogen to sustain glucose as the primary fuel source in brain by enhancing glucose transport, uptake and aerobic glycolysis (oxidative phosphorylation coupled to pyruvate metabolism) is likely linked to its ability to prevent age-associated metabolic decline in brain and thus could be a key mechanism whereby estrogen reduces the risk of AD in postmenopausal women [1, 6, 19–24].

Reproductive senescence is a multifactorial process with a high degree of interpersonal variability and subject to a host of beneficial or detrimental influences. As such, reproductive senescence is an illustrative example of both the aging process and of modifiers of aging, such as ovarian hormone status, which both contribute to alteration in brain metabolic profile. In the current study, we sought to determine the impact of loss of ovarian hormones associated with reproductive senescence on mitochondrial function, particularly mitochondrial bioenergetics. We further investigate the individual variability in metabolic profile during the reproductive senescence transition. The results presented demonstrate that loss of ovarian hormones during reproductive senescence parallels the accelerated decline in mitochondrial bioenergetics, linking the loss of ovarian hormones to the development of a hypometabolic brain phenotype which could be clinically relevant to the in prodromal phase of AD. Collectively current clinical findings and findings from this study provide a plausible mechanism of increased AD risk in menopausal women.

2. Materials and Methods

2.1 Transgenic Mice

Colonies of 3xTgAD and nonTg mouse strain (C57BL6/129S;Gift from Dr. Frank Laferla, University of California, Irvine)[25] were bred and maintained at the University of Southern California (Los Angeles, CA) following National Institutes of Health guidelines on use of laboratory animals and an approved protocol by the University of Southern California Institutional Animal Care and Use Committee. Mice were housed on 12 h light/dark cycles and provided *ad libitum* access to food and water. Only intact female mice at the age of 3, 6, 9, and 12 months were used for the experiments.

2.2 Brain Tissue Preparation and Mitochondrial Isolation

Intact female mice of both 3xTg-AD and nonTg groups at different age groups (3, 6, 9, and 12 months) were sacrificed by decapitation and the brains were quickly dissected on ice.

Cerebellum and brain stem was removed from each brain and the hippocampus within the left hemisphere was harvested. Brain mitochondria were isolated from the remainder (whole brain minus cerebellum and brain stem) following previously established protocol [26]. The brain was rapidly minced and homogenized at 4°C in mitochondrial isolation buffer (MIB) (PH 7.4), containing sucrose (320 mM), EDTA (1 mM), Tris-HCl (10mM), and Calbiochem's Protease Inhibitor Cocktail Set I (AEBSF-HCl 500μM, aprotinin 150 nM, E-64 1 μM, EDTA disodium 500 μM, leupeptin hemisulfate 1 μM). Single-brain homogenates were then centrifuged at $1500 \times g$ for 5 min. The pellet was resuspended in MIB, rehomogenized, and centrifuged again at $1500 \times g$ for 5 min. The postnuclear supernatants from both centrifugations were combined, and crude mitochondria were pelleted by centrifugation at $21,000 \times g$ for 10 min. The resulting mitochondrial pellet was resuspended in 15% Percoll made in MIB, layered over a preformed 23%/40% Percoll discontinuous gradient, and centrifuged at $31,000 \times g$ for 10 min. The purified mitochondria were collected at the 23%/40% interface and washed with 10 ml MIB by centrifugation at $16,700 \times g$ for 13 min. The loose pellet was collected and transferred to a microcentrifuge tube and washed in MIB by centrifugation at $9000 \times g$ for 8 min. The resulting mitochondrial pellet was resuspended in MIB to an approximate concentration of 1mg/ml. The resulting mitochondrial samples were used immediately for respiratory measurements and hydrogen peroxide production or stored at −80°C for later protein and enzymatic assays. During mitochondrial purification, aliquots were collected for confirmation of mitochondrial purity and integrity, Western blot analysis was performed for mitochondrial anti-VDAC (1:500; Mitosciences, Eugene, OR), nuclear anti-histone H1 (1:250; Santa Cruz Biotechnology, Santa Cruz, CA), endoplasmic reticulum anti-calnexin (1:2000, SPA 865; Stressgen, now a subsidiary of Assay Designs, Ann Arbor, MI), and cytoplasmic anti-myelin basic protein (1:500, clone 2; RDI, Concord, MA) (data not shown).

2.3 Respiratory Measurement

Mitochondrial oxygen consumption was measured polarographically using a Clarke-type electrode. 100 μg of isolated mitochondria were placed in the respiration chamber at 37°C in respiratory buffer (130 mM KCl, 2 mM KH_2PO_4, 3mM HEPES, 2mM $MgCl_2$, 1 mM EGTA) to yield a final concentration of 200 μg/mL After a 1 min baseline recording, mitochondria were energized by the addition of glutamate (5 mM) and malate (5 mM) as substrates. State 3 respiration was stimulated by the addition of ADP (410 μM). State 4_0 respiration was induced by the addition of three pulses of the adenine nucleotide translocator (ANT) inhibitor atractyloside (50 μM) to deplete ADP. The rate of oxygen consumption was calculated based on the slope of the response of isolated mitochondria to the successive administration of substrates. The respiratory control ratio (RCR) was defined by dividing the rate of oxygen consumption/min for state 3 (presence of ADP) by the rate of oxygen consumption/min for state 4_0 respiration (Absence of ADP by addition of atractyloside).

2.4 Enzyme Activity Assay

PDH activity was measured by monitoring the conversion of NAD+ to NADH by following the change in absorption at 340 nm as previously described [27]. Isolated brain mitochondria were dissolved in 2% CHAPS buffer to yield a final concentration of 15 μg/μl and incubated at 37°C in PDH Assay Buffer (35mM KH_2PO_4, 2 mM KCN, 0.5 mM EDTA, 5 mM $MgCl_2$, (pH 7.25 with KOH), 200mM Sodium Pyruvate, 2.5 mM Rotenone, 4mM Sodium CoA, 40 mM TPP). The reaction was initiated by the addition of 15mM NAD^+. COX activity was measured on isolated mitochondria (20 μg) using Rapid Microplate Assay kit for Mouse Complex IV Activity (Mitosciences, Eugene, OR) following the manufacturer's instructions.

2.5 Lipid Peroxidation

Lipid peroxides in brain mitochondria and hippocampal lysates were measured using the leucomethylene blue assay [28], using *tert*-butyl hydroperoxide as a standard, by monitoring the 650nm absorbance after 1 h incubation at RT. The aldehyde product or termination production of lipid peroxidation in brain mitochondria was determined by measuring thiobarbituric acid reactive substances (TBARS). Samples were mixed with 0.15 M phosphoric acid. After the addition of thiobarbituric acid, the reaction mixture was heated to 100°C for 1 h. After cooling and centrifugation, the formation of TBARS was determined by the absorbance of the chromophore (pink dye) at 531 nm using 600nm as the reference wavelength.

2.6 Western Blot Analysis

Protein concentrations were determined by using the BCA protein assay kit (Pierce, Rockford, IL). Equal amounts of mitochondrial proteins (20 μg/well) were loaded in each well of a 15% SDS-PAGE gel, electrophoresed with a Tris/glycine running buffer, and transferred to a 0.45 μm pore size polyvinylidene difluoride (PVDF) membrane and immunoblotted with SCOT antibody (1:100, Santa Cruz, CA), HADHA antibody (1:1000, abcam, Cambridge, MA), and porin/VDAC antibody (1:500, Mitosciences, Eugene, OR). HRP-conjugated anti-rabbit antibody and HRP-anti-mouse antibody (Vector Laboratories, Burlingame, CA) were used as secondary antibodies. Immunoreactive bands were visualized by Pierce SuperSignal Chemiluminescent Substrates (Thermo Scientific) and captured by Molecular Imager ChemiDoc XRS System (Bio-Rad, Hercules, CA). All band intensities were quantified using Un-Scan-it software.

2.7 Statistics

Statistically significant differences between groups were determined by an ANOVA followed by a Newman-Keuls post-hoc analysis.

3. Results

In the process of conducting an analysis of bioenergetic changes in aging to determine if changes in mitochondrial preceded development of AD pathology, we observed that a decline in bioenergetics occurred after the development of AD pathology but which corresponded to the transition of reproductive senescence. Data presented in Figures 1, 2, 4 and 5 are derived from the quantitative data presented in Figure 4 and Table 1 of the PNAS manuscript [7]. In the previous publication the emphasis was on changes that occur prior to development of AD pathology in the 3xTgAD female mouse brain. In this report, we focus on the bioenergetic changes that occur during the reproductive senescent period in the normal nonTg mouse brain not associated with AD pathology and in the 3xTgAD female mouse brain in the presence of AD pathology.

3.1 Reproductive senescence paralleled significant decrease in mitochondrial respiration

To investigate the impact of reproductive senescence on mitochondrial bioenergetic aging profile, mitochondrial respiration was determined in freshly isolated whole forebrain mitochondria from female 3xTg-AD and nonTg mice at 3, 6, 9 and 12 months of age. Respiratory rate of isolated whole brain mitochondria was first determined using glutamate (5 mM) and malate (5 mM) as respiratory substrates. ADP addition to the mitochondrial suspension initiated state 3 respiration. Addition of the adenine nucleotide transporter inhibitor atractyloside reduced the rate of O_2 consumption to that of state 4_o respiration, limited by proton permeability of the inner membrane. In both nonTg and 3xTgAD group, there was a moderate age-related decline in the respiratory control ratio (RCR; state 3: state

4_o) from 3 month to 9 month, with 3xTgAD mice exhibiting lower RCR compared to age-matched nonTg group. More importantly, reproductive senescence paralleled a significant decline in mitochondrial respiration in nonTg mice, and dramatically exacerbated the deficit in mitochondrial respiration in 3xTgAD mice (Fig. 1).

3.2 Accelerated decline in metabolic enzyme activity with reproductive senescence

Changes in mitochondrial respiration could be attributed to alteration in metabolic enzyme activities. Pyruvate dehydrogenase (PDH) is the key enzyme linking glycolysis to oxidative phosphorylation (OXPHOS); Complex IV, cytochrome c oxidase (COX) is the terminal enzyme of electron flow and reduces O_2 to H_2O. Decreased expression and activity of COX and PDH have been observed in postmortem brain tissue derived from Alzheimer's patients [28]. To investigate the impact of reproductive senescence on PDH and COX activity, we assessed PDH and COX activity in mitochondria isolated from whole forebrain of the same set of 3xTg-AD and nonTg mice utilized for the mitochondrial respiration. Similary to our previous findings[7], 3xTgAD mice had significant lower PDH and COX activity compared to age-matched nonTg mice at 9 and 12 month. More importantly, in both nonTg and 3xTgAD mice, reproductive senescence paralleled a significant decline in PDH and COX activity (Fig. 2A&B). PDH is the key rate-limiting enzyme in mitochondria to convert pyruvate, the end product of glycolysis, into acetyl-CoA, which subsequently condenses with oxaloacetate to initiate the TCA cycle for energy production. The decline in enzyme activity, particularly accelerated decline in PDH activity with reproductive senescence indicates diminished metabolism of glucose for ATP production.

3.3 Increased enzyme expression in ketogenic pathway with reproductive senescence

Decreased glucose metabolism for ATP production could activate alternative metabolic pathways to compensate for decreased PDH activity. Brain, under long term starvation or certain disease conditions, could use ketone bodies as an alternative fuel source [8, 29–30]. To investigate whether reproductive senescence leads to a ketogenic brain metabolic profile, we determined the expression of enzymes involved in ketone generation and utilization. HADHA, hydroxyacyl-Coenzyme A dehydrogenase/3-ketoacyl-Coenzyme A thiolase/enoyl-Coenzyme A hydratase (trifunctional protein), alpha subunit, catalyzes the last three steps of mitochondrial beta-oxidation of long chain fatty acids and is involved in ketogenesis. SCOT, 3-oxoacid-CoA transferase 1, catabolizes ketone bodies to generate Acetyl-CoA, which is subsequently used for ATP generation. 3xTgAD mice exhibited significantly higher HADHA and SCOT expression at 3 months of age relative to nonTg mice, indicating activation of ketogenic pathway to compensate for the deficit in mitochondrial bioenergetics that occurred early in AD [7]. The decline in HADHA and SCOT expression with age in 3xTgAD from 3 month to 9 month indicates that the compensatory ketogenic pathway is transient. More importantly, reproductive senescence paralleled a significant increase in HADHA expression in both nonTg and 3xTgAD mice (Fig. 3B). NonTg mice also exhibited significant increase in SCOT expression with reproductive senescence with 3xTgAD exhibiting a similar but not significant increase in SCOT (Fig. 3A). Collectively, these data indicate that in the normal nonTg brain, enzymes required for generation and metabolism of ketone bodies significantly increased during reproductive senescence. In 3xTgAD brain, utilization of ketones is limited due to the modest increase in SCOT expression despite the significant up-regulation of enzymes involved in long-chain and short chain fatty acid oxidation, including HADHA and SCHAD [7].

3.4 Oxidative Stress is mainly associated with aging rather than reproductive senescence

Mitochondrial dysfunction is associated with oxidative stress and development of AD neuropathology. To investigate the impact of reproductive senescence on the oxidative load

of brain mitochondria, we assessed the magnitude of lipid peroxidation in mitochondria isolated from whole forebrain of female 3xTg-AD and nonTg mice at 3, 6, 9 and 12 months of age. Consistent with previously findings, 3xTgAD mice exhibited higher level of lipid peroxide relative to age-matched nonTg mice at all age groups, indicating increased oxidative stress associated with Alzheimer's progression. However, unlike mitochondrial bioenergetics, both nonTg and 3xTgAD mice exhibited a rather steady age-dependent rate of increase in lipid peroxidation with no significant change in rate of increase during reproductive senescence (Fig. 4), suggesting that the increase in oxidative stress, at least increase in lipid peroxidation, is largely age-dependent.

3.5 Bioenergetic phenotypes emerge from the reproductive senescence transition

Aside from the general decline in mitochondrial bioenergetics paralleled reproductive senescence, we also observed segregation of the bioenergetic profiles in individual mice during the reproductive transition. In nonTg and 3xTgAD mice, PDH activity exhibited similar degree of variability through 9 month and 12 month (Fig. 5A). COX activity, in contrast, exhibited relatively larger variability at 9 month in both nonTg and 3xTgAD mice, whereas at 12 month COX activity values were tightly clustered in both groups (Fig. 5B).

4. Discussion

Increasing evidence links mitochondrial dysfunction in multiple neurodegenerative disorders, such as Alzheimer's disease (AD) [11]. We previously demonstrated that mitochondrial bioenergetic deficits precede AD pathology in the female triple transgenic AD mouse model [7], suggesting a potential causal role of mitochondrial bioenergetic deficiency in AD pathogenesis. Clinically, Alzheimer's pathology is accompanied by a decrease in expression and activity of enzymes involved in mitochondrial bioenergetics, which would be expected to lead to compromised electron transport chain complex activity and reduced ATP synthesis [28]. Further, in AD there is a generalized shift from glycolytic energy production towards use of an alternative fuel, ketone bodies. This is evidenced by a 45% reduction in cerebral glucose utilization in AD patients [31], which is paralleled by decrease in the expression of glycolytic enzymes coupled to a decrease in the activity of the pyruvate dehydrogenase complex [28]. In the current study, reproductive senescent nonTg female mice exhibited a brain metabolic profile comparable to the metabolic phenotype observed early in AD. In normal aging female nonTg mice, reproductive senescence paralleled a significant decline in mitochondrial bioenergetic function including decreased mitochondrial respiration, compromised PDH and COX activity, and activation of ketogenic pathway. In 3xTgAD mice, reproductive senescence paralleled the exacerbation of the existing impairment of mitochondrial bioenergetics that occurred early in the disease progression.

PDH is the key rate-limiting enzyme in mitochondria to convert pyruvate, the end product of glycolysis, into acetyl-CoA, which subsequently condenses with oxaloacetate to initiate the TCA cycle for energy production. Complex IV is the terminal enzyme of electron flow and reduces O_2 to H_2O. Compromised activity of PDH and COX reduces the substrate input and driving force for oxidative phosphorylation, resulting in increased ATP demand via other pathways that leads to the activation of ketogenic pathway. Our findings of decreased activity of PDH and COX with reproductive senescence are consistent with the clinical observation of significantly decreased PDH and COX activity in postmortem Alzheimer's brain tissue [28, 32].

In contrast to decreased PDH and COX activity, reproductive senescence paralleled a significant increase in HADHA and SCOT protein expression in nonTg mice and a moderate increase in 3xTgAD mice, indicative of activation of ketogenic pathway in brain which would be required to generate an alternative fuel source to compensate for the decline in

glucose driven metabolic activity. These findings are also consistent with clinical observations that patients with incipient AD exhibit a utilization ratio of 2:1 glucose to alternative fuel whereas comparably aged controls exhibit a ratio of 29:1 while young controls exclusively use glucose as with a ratio of 100:0 ratio [33].

Together, these data indicate a critical role for ovarian hormones in sustaining and enhancing glucose driven brain metabolism and mitochondrial function. Ovarian hormones, particularly estrogen, has been demonstrated to positively enhance glucose driven mitochondrial bioenergetics [34]. Estrogen promotes the coupling of glycolysis to oxidative phosphoyrlation (OXPHOS) by increasing the activity of both glycolytic enzymes, including hexokinase, phosphofructokinase, and phosphoglycerate kinase [35], and the expression and activity of proteins involved in OXPHOS, including pyruvate dehydrogenase, aconitase, and ATP synthase [19]. Loss of ovarian hormones due to reproductive senescence could induce a systematic decrease in glucose driven ATP generation. The increase in ketogenic enzyme expression is reflective of compensatory mechanism to generate an alternative pathway to utilize ketone body for ATP generation. Noticeably, at 12 month nonTg mice expressed significantly higher level of SCOT relative to 3xTgAD mice but which were commensurate with SCOT levels at the early preAD pathology stage of AD. Collectively, findings from this study indicate that loss of ovarian hormones due to reproductive senescence accompanies a bioenergetic phenotype in the female brain suggestive of the prodromal AD metabolic phenotype. These findings provide a potential mechanism underlying increased risk for AD observed in postmenopausal women.

To assess whether all reproductively senescing mice bioenergetically aged the same, we analyzed the bioenergetic responses from individual nonTg and 3xTgAD mice. Results of this analysis, indicated segregation of metabolic profiles among individual mice through reproductive senescence transition. The variability of PDH remains largely the same throughout reproductive senescence (Fig 5A). Consistent with our previous findings that decline in PDH expression occurred early in 3xTgAD female mouse brain [7], data from this study indicate that compromised PDH associated with loss of ovarian hormones in reproductive senescence likely induces a variety of adaptive responses, including activation of ketogenic pathway and fatty acid oxidation, to compensate for the loss of substrate availability. COX activity, in contrast, showed greater variability between individual mice at the onset of reproductive senescence in both nonTg and 3xTgAD mice at 9 month (Fig. 5B). However, variability in COX activity collapsed at 12 month, when mice are reproductively senescent, and converged to cluster at a much reduced level of activity. These data indicated that despite the compensatory pathways that supply alternative substrates, the net catalytic reactivity and energy transducing capacity relies stringently on COX activity as COX serves as the terminal point of electron transport. Although the variance in COX activity at earlier stage likely reflects the differential adaptation of compensatory pathways, the convergent collapse in COX activity at 12 month likely indicates a point of no return as far as energy generation by mitochondria is concerned. However, the decline between 9 and 12 month opens a therapeutic, if not a preventative, window to alleviate the detrimental impact of loss of ovarian hormones on bioenergetics during reproductive senescence.

Collectively, findings from this study demonstrate that reproductive senescence is paralleled by a significant decline in bioenergetics and mitochondrial function in normal nonTg mice and the exacerbation of the impaired mitochondrial bioenergetics pre-existed in 3xTgAD mice. These data indicate that reproductive senescence might accelerate the decline in mitochondrial bioenergetics, linking reproductive senescence to the development of a hypometabolic brain phenotype clinically observed in prodromal AD brains [36]. Further, multiple bioenergetic metabolic phenotypes evident at the onset of reproductive senescence indicates the activation of a combination of adaptive responses. Together with our previous

findings that mitochondrial bioenergetic deficits precede AD pathology, the current study provides a plausible mechanism underlying the increased risk for AD in menopausal women and importantly indicates a critical window of opportunity to prevent development of bioenergetic phenotype of AD.

Acknowledgments

Abbreviations

AD	Alzheimer's disease
3xTgAD	triple transgenic Alzheimer's disease
nonTg	non-transgenic
E2	17β-estradiol
PDH	pyruvate dehydrogenase
COX	cytochrome c oxidase

References

1. Brinton RD. The healthy cell bias of estrogen action: mitochondrial bioenergetics and neurological implications. Trends in neurosciences. 2008; 31:529–537. [PubMed: 18774188]

2. Magistretti PJ. Neuron-glia metabolic coupling and plasticity. J Exp Biol. 2006; 209:2304–2311. [PubMed: 16731806]

3. Wallace DC. A mitochondrial paradigm of metabolic and degenerative diseases, aging, and cancer: a dawn for evolutionary medicine. Annu Rev Genet. 2005; 39:359–407. [PubMed: 16285865]

4. Swerdlow RH. The Neurodegenerative Mitochondriopathies. J Alzheimers Dis. 2009

5. Mattson MP. Pathways towards and away from Alzheimer's disease. Nature. 2004; 430:631–639. [PubMed: 15295589]

6. Brinton RD. Estrogen regulation of glucose metabolism and mitochondrial function: therapeutic implications for prevention of Alzheimer's disease. Adv Drug Deliv Rev. 2008; 60:1504–1511. [PubMed: 18647624]

7. Yao J, Irwin RW, Zhao L, Nilsen J, Hamilton RT, Brinton RD. Mitochondrial bioenergetic deficit precedes Alzheimer's pathology in female mouse model of Alzheimer's disease. Proceedings of the National Academy of Sciences of the United States of America. 2009; 106:14670–14675. [PubMed: 19667196]

8. Costantini LC, Barr LJ, Vogel JL, Henderson ST. Hypometabolism as a therapeutic target in Alzheimer's disease. BMC Neurosci. 2008; 9(Suppl 2):S16. [PubMed: 19090989]

9. Wang X, Su B, Perry G, Smith MA, Zhu X. Insights into amyloid-beta-induced mitochondrial dysfunction in Alzheimer disease. Free Radic Biol Med. 2007; 43:1569–1573. [PubMed: 18037122]

10. Blalock EM, Chen KC, Sharrow K, Herman JP, Porter NM, Foster TC, Landfield PW. Gene microarrays in hippocampal aging: statistical profiling identifies novel processes correlated with cognitive impairment. J Neurosci. 2003; 23:3807–3819. [PubMed: 12736351]

11. Blalock EM, Geddes JW, Chen KC, Porter NM, Markesbery WR, Landfield PW. Incipient Alzheimer's disease: microarray correlation analyses reveal major transcriptional and tumor suppressor responses. Proceedings of the National Academy of Sciences of the United States of America. 2004; 101:2173–2178. [PubMed: 14769913]

12. Reiman EM, Chen K, Alexander GE, Caselli RJ, Bandy D, Osborne D, Saunders AM, Hardy J. Functional brain abnormalities in young adults at genetic risk for late-onset Alzheimer's dementia. Proc Natl Acad Sci U S A. 2004; 101:284–289. [PubMed: 14688411]

13. Rowe WB, Blalock EM, Chen KC, Kadish I, Wang D, Barrett JE, Thibault O, Porter NM, Rose GM, Landfield PW. Hippocampal expression analyses reveal selective association of immediate-early, neuroenergetic, and myelinogenic pathways with cognitive impairment in aged rats. J Neurosci. 2007; 27:3098–3110. [PubMed: 17376971]

14. Moreira PI, Santos MS, Seica R, Oliveira CR. Brain mitochondrial dysfunction as a link between Alzheimer's disease and diabetes. J Neurol Sci. 2007; 257:206–214. [PubMed: 17316694]

15. Miller JA, Oldham MC, Geschwind DH. A systems level analysis of transcriptional changes in Alzheimer's disease and normal aging. J Neurosci. 2008; 28:1410–1420. [PubMed: 18256261]

16. Mosconi L, Tsui WH, Herholz K, Pupi A, Drzezga A, Lucignani G, Reiman EM, Holthoff V, Kalbe E, Sorbi S, Diehl-Schmid J, Perneczky R, Clerici F, Caselli R, Beuthien-Baumann B, Kurz A, Minoshima S, de Leon MJ. Multicenter Standardized 18F-FDG PET Diagnosis of Mild Cognitive Impairment, Alzheimer's Disease, and Other Dementias. J Nucl Med. 2008; 49:390–398. [PubMed: 18287270]

17. Liang WS, Dunckley T, Beach TG, Grover A, Mastroeni D, Ramsey K, Caselli RJ, Kukull WA, McKeel D, Morris JC, Hulette CM, Schmechel D, Reiman EM, Rogers J, Stephan DA. Altered neuronal gene expression in brain regions differentially affected by Alzheimer's Disease: A reference data set. Physiol Genomics. 2008

18. Mosconi L, Brys M, Switalski R, Mistur R, Glodzik L, Pirraglia E, Tsui W, De Santi S, de Leon MJ. Maternal family history of Alzheimer's disease predisposes to reduced brain glucose metabolism. Proc Natl Acad Sci U S A. 2007; 104:19067–19072. [PubMed: 18003925]

19. Nilsen J, Irwin RW, Gallaher TK, Brinton RD. Estradiol in vivo regulation of brain mitochondrial proteome. J Neurosci. 2007; 27:14069–14077. [PubMed: 18094246]

20. Henderson, VaB. RD Menopause and Mitochondria: Windows into Estrogen Effects on Alzheimer's Disease Risk and Therapy: Progress in Brain Research Neuroendocrinology. 2010 In press.

21. Hogervorst E, Yaffe K, Richards M, Huppert FA. Hormone replacement therapy to maintain cognitive function in women with dementia. Cochrane database of systematic reviews (Online). 2009:CD003799. [PubMed: 19160224]

22. Morrison JH, Brinton RD, Schmidt PJ, Gore AC. Estrogen, menopause, and the aging brain: how basic neuroscience can inform hormone therapy in women. J Neurosci. 2006; 26:10332–10348. [PubMed: 17035515]

23. Rocca WA, Bower JH, Maraganore DM, Ahlskog JE, Grossardt BR, de Andrade M, Melton LJ Iii. Increased risk of cognitive impairment or dementia in women who underwent oophorectomy before menopause. Neurology. 2007

24. Yaffe K. Hormone therapy and the brain: deja vu all over again? Jama. 2003; 289:2717–2719. [PubMed: 12771119]

25. Oddo S, Caccamo A, Shepherd JD, Murphy MP, Golde TE, Kayed R, Metherate R, Mattson MP, Akbari Y, LaFerla FM. Triple-transgenic model of Alzheimer's disease with plaques and tangles: intracellular Abeta and synaptic dysfunction. Neuron. 2003; 39:409–421. [PubMed: 12895417]

26. Irwin RW, Yao J, Hamilton RT, Cadenas E, Brinton RD, Nilsen J. Progesterone and estrogen regulate oxidative metabolism in brain mitochondria. Endocrinology. 2008; 149:3167–3175. [PubMed: 18292191]

27. Gohil K, Jones DA. A sensitive spectrophotometric assay for pyruvate dehydrogenase and oxoglutarate dehydrogenase complexes. Biosci Rep. 1983; 3:1–9. [PubMed: 6839008]

28. Blass JP, Sheu RK, Gibson GE. Inherent abnormalities in energy metabolism in Alzheimer disease. Interaction with cerebrovascular compromise. Ann N Y Acad Sci. 2000; 903:204–221. [PubMed: 10818509]

29. Guzman M, Blazquez C. Ketone body synthesis in the brain: possible neuroprotective effects. Prostaglandins, leukotrienes, and essential fatty acids. 2004; 70:287–292.

30. Morris AA. Cerebral ketone body metabolism. J Inherit Metab Dis. 2005; 28:109–121. [PubMed: 15877199]

31. Ishii K, Sasaki M, Kitagaki H, Yamaji S, Sakamoto S, Matsuda K, Mori E. Reduction of cerebellar glucose metabolism in advanced Alzheimer's disease. J Nucl Med. 1997; 38:925–928. [PubMed: 9189143]

32. Martins RN, Hallmayer J. Age at onset: important marker of genetic heterogeneity in Alzheimer's disease. Pharmacogenomics J. 2004; 4:138–140. [PubMed: 15024381]

33. Hoyer S. Abnormalities of glucose metabolism in Alzheimer's disease. Ann N Y Acad Sci. 1991; 640:53–58. [PubMed: 1776759]

34. Brinton RD. The healthy cell bias of estrogen action: mitochondrial bioenergetics and neurological implications. Trends Neurosci. 2008; 31:529–537. [PubMed: 18774188]

35. Kostanyan A, Nazaryan K. Rat brain glycolysis regulation by estradiol-17 beta. Biochim Biophys Acta. 1992; 1133:301–306. [PubMed: 1531302]

36. Reiman EM. Linking brain imaging and genomics in the study of Alzheimer's disease and aging. Ann N Y Acad Sci. 2007; 1097:94–113. [PubMed: 17413015]
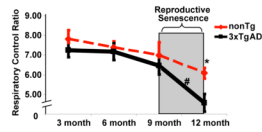
Figure 1. Reproductive senescence paralleled a significant decline in mitochondrial respiration
Whole brain mitochondria were isolated from intact female mice and state 3/state 4 respiration was determined. Oxygen electrode measurements of respiration using isolated brain mitochondria from 3xTg-AD and nonTg mice were conducted in the presence of L-malate (5 mM), L-glutamate (5 mM), ADP (410 μM) to initiate state 3 respiration, and atractyloside to induce state 4o respiration. Bars represent the mean ± S.E.M. of the respiratory control ratio (RCR, state3/state 4 respiration) (*=p<0.05 compared between 3xTgAD group and age-matched nonTg group; #=p<0.05 compared between different age group within the same genotype, n=6)
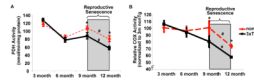
Figure 2. Reproductive senescence paralleled a significant decline in PDH and COX activity
Brain mitochondria isolated from both nonTg and 3xTg-AD mice were assessed for PDH (A) and COX (B) activity. Relative COX Activity was presented as the relative value normalized to that of 3 month nonTg female mice. Mean ± SEM (*=p<0.05 as compared to age-matched nonTg group; #=p<0.05 compared between different age group within the same genotype, n=6).
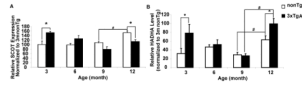
Figure 3. Increased enzyme expression in ketogenic pathway with reproductive senescence
Both female nonTg and 3xTgAD mice at 3, 6, 9, and 12 months of age were sacrificed and
mitochondrial SCOT and HADHA level were determined by western blot. A, age profile of
SCOT expression in nonTg and 3xTgAD mice; B, age profile of HADHA expression in
nonTg and 3xTgAD mice. (*=p<0.05 as compared to age-matched nonTg group; #=p<0.05
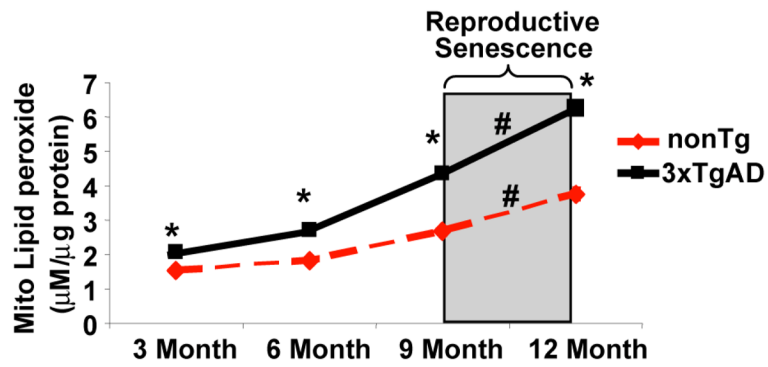compared between different age group within the same genotype, n=6).

Figure 4. Reproductive senescence does not accelerate increase in oxidative stress
Whole brain mitochondria were isolated from intact female mice and lipid peroxide levels were determined by the leucomethylene blue assay. Bars represent mean ± S.E.M. (*=$p<0.05$ compared with age-matched nonTg group; #=$p<0.05$ compared between different age group within the same genotype, n=6).
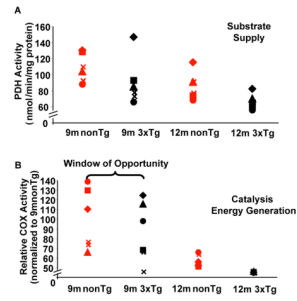
Figure 5. Bioenergetic phenotypes emerge during reproductive senescence transition
Brain mitochondria isolated from both nonTg and 3xTg-AD mice were assessed for PDH
activity (A) and COX activity (B). Individual values for PDH and COX activity derived
were plotted in scatter plot format.